

# Study of the Pressure–Time–Temperature Transformation of Amorphous $\text{La}_6\text{Ni}_5\text{Al}_{89}$ by the Energy Dispersive Method for Phase Transition

Barbara Paci,<sup>\*,†</sup> Valerio Rossi-Albertini,<sup>†</sup> Marcin Sikorski,<sup>‡</sup> Wojciech Roseker,<sup>‡</sup>  
Dong Qian,<sup>‡</sup> and J. Z. Jiang<sup>‡,§</sup>

*Istituto di Struttura della Materia-CNR, Area della Ricerca di Roma Tor Vergata, Via Fosso del cavaliere 100, 00133 Rome, Italy, Department of Physics, Building 307, Technical University of Denmark, DK-2800 Lyngby, Denmark, and Laboratory of New-Structured Materials, Department of Materials Science and Engineering, Zhejiang University, Hangzhou 310027, P.R. China*

Received July 15, 2005. Revised Manuscript Received September 13, 2005

An energy dispersive X-ray diffraction method to observe phase transitions is applied to follow the crystallization of an amorphous alloy ( $\text{La}_6\text{Ni}_5\text{Al}_{89}$ ) in isothermal conditions. In this way, the diffraction-based configurational entropy (DCE) of the system undergoing the phase transformations was measured and the curves describing the transitions, qualitatively equivalent to a differential scanning calorimetry (DSC) thermogram, could be drawn. Finally, the analysis of such curves allowed calculation of some points of the alloy pressure–time–temperature transformation (PTTT) diagram. More importantly, the present work shows that the DCE method can be successfully applied even when DSC can no longer be used. As a consequence, regions of the phase diagram that could not be reached up to now become accessible, opening the way to the study of transition phenomena under extreme conditions.

## 1. Introduction

In this work an original diffraction-based technique, recently proposed for studying phase transitions, is used. Such technique was validated in a previous paper,<sup>1</sup> comparing the results obtained for polymer phase transitions with the ones obtained by DSC, performed under the same conditions, therefore demonstrating that the information obtained is equivalent in the two cases.

The energy dispersive X-ray diffraction method to observe phase transitions (EDXD-PT) technique shows its full potentialities when used in nonstandard thermodynamic conditions, such as high pressure or temperature.

Indeed, while no calorimeter could stand the high pressures at which the samples are submitted in this study, the DCE measurements carried out by EDXD-PT (and a tungsten carbide anvil cell) provide an easy way to gain the information required. Moreover, the intense heating of the sample, which would make the DSC heat flux measurement unreliable, represents a minor difficulty only for EDXD-PT, consisting of a simple Debye–Waller-like correction (thermal expansion is already taken into account in data processing). Finally, in EDXD-PT, very small samples, which would give undetectably weak DSC signals, can be utilized. This would enable one to use diamond anvil cells, to observe the phase transition characteristics in unprecedented conditions.

Here we apply the EDXD-PT method to the study of an amorphous alloy submitted to high-temperature/–pressure conditions, demonstrating experimentally its ability to describe the entropy changes in a typical case for which no DSC data are available. The alloy  $\text{La}_6\text{Ni}_5\text{Al}_{89}$  was chosen as a test sample since the Al-based amorphous alloys with an Al concentration of about 90 at. % have attracted much attention due to their novel mechanical properties.<sup>2,3</sup> Indeed, the mechanical properties of partially crystallized amorphous alloys with nanometer-sized Al crystals are enhanced,<sup>4–6</sup> making this new family of Al-based alloys promising candidates as advanced engineering materials. Because of the high critical cooling rates required, these alloys are normally prepared either in the form of thin ribbons or as powders. However, for most engineering applications, the amorphous ribbons or powders are consolidated to form bulk materials.<sup>5,7</sup> One of the fundamental issues in the consolidation process is the effect of pressure on the thermal stability of the amorphous phase.<sup>8,9</sup> This is a critical point for optimizing the consolidation parameters for obtaining bulk

- (2) He, Y.; Poon, S. J.; Shiflet, G. J. *Science* **1988**, *241*, 1640. Shiflet, G. J.; He, Y.; Poon, S. J. *J. Appl. Phys.* **1988**, *64*, 6863.
- (3) Inoue, A.; Ohtera, K.; Tsai, A. P.; Masumoto, T. *Jpn. J. Appl. Phys.* **1998**, *27*, L280; *27*, L479.
- (4) Chen, H.; He, Y.; Shiflet, G. J.; Poon, S. J. *Scr. Metall. Mater.* **1991**, *25*, 1421.
- (5) Kim, Y. H.; Inoue, A.; Masumoto, T. *Mater. Trans. JIM* **1991**, *32*, 331. Inoue, A.; Kimura, H. *Mater. Sci. Forum* **1997**, *235–238*, 873. Inoue, A. *Prog. Mater. Sci.* **1998**, *43*, 365.
- (6) Gloriant, T.; Greer, A. L. *Nanostruct. Mater.* **1998**, *10*, 389. Zhong, Z. C.; Greer, A. L. *Intr. J. Non-equ. Proc.* **1998**, *11*, 35.
- (7) Zhou, F.; Zhang, X. H.; Lu, K. J. *Mater. Res.* **1998**, *13*, 784.
- (8) Zhuang, Y. X.; Jiang, J. Z.; Zhou, T. J.; Rasmussen, H.; Gerward, L.; Mezouar, M.; Crichton, W.; Inoue, A. *Appl. Phys. Lett.* **2000**, *77*, 4133.
- (9) Zhuang, Y. X.; Jiang, J. Z.; Lin, Z. G.; Mezouar, M.; Crichton, W.; Inoue, A. *Appl. Phys. Lett.* **2001**, *79*, 743.

\* To whom correspondence should be addressed. Tel.: +39-0649934174. Fax: +39-064993153. E-mail: barbara.paci@ism.cnr.it

<sup>†</sup> Istituto di Struttura della Materia-CNR.

<sup>‡</sup> Technical University of Denmark.

<sup>§</sup> Zhejiang University.

(1) Rossi-Albertini, V.; Isopo, A.; Caminiti, R.; Tentolini, U. *Appl. Phys. Lett.* **2002**, *80*, 775.

samples with the desired structure and properties. Therefore, such an alloy is the ideal system to show the EDXD-PT qualities (at high pressure and temperature) to their full extent.

From the results of the DCE measurements—obtained applying the energy dispersive X-ray diffraction<sup>10</sup> method to observe phase transitions<sup>11</sup> (EDXD-PT)—curves equivalent to the DSC thermograms are obtained, whose maxima (minima) represent the exothermal (endothermic) transitions. The equivalence of DSC and DCE is due to the fact that both techniques are sensitive to the change of the system entropy during the phase transitions. Indeed, in the former case, the heat flux released or absorbed by the sample can be used to calculate the change in the entropy according to the Carnot *thermodynamic* definition (because of the proportionality between enthalpy and entropy when the temperature is fixed). In the latter, the Fourier transform of the diffraction patterns (pair correlation function) can be used to calculate the change in the entropy according to the Gibbs ensemble-invariant definition of entropy in *statistical mechanics*.<sup>12,13</sup>

However, since the DSC method works best at high heating rates, while the DCE is best at low heating rates, the latter is more reliable when quasi-static phase transitions are studied. The very low heating rates that can be held in diffraction measurements guarantee that the thermal perturbation to the system can be arbitrarily reduced and the thermodynamic (quasi) equilibrium conditions can be approached. A last remark concerns the use of the energy-dispersive mode<sup>14,15</sup> rather than its conventional angular dispersive (AD) counterpart: on one hand, the EDXD does not require any movement during data (fixed geometry setup) and, on the other hand, a single diffraction angle is sufficient to collect the pattern, instead of the wide angular interval required in the AD mode, which may be hardly accessible due to the geometric constrains of the high-pressure cells.

## 2. Experimental Section

Ingots, with a nominal composition  $\text{La}_6\text{Ni}_5\text{Al}_{89}$ , were prepared by arc-melting a mixture of pure Al (99.99 wt %), La (99.9 wt %), and Ni (above 99.96 wt %) in a purified argon atmosphere. Amorphous ribbons ( $\sim 1.3 \times 0.02 \text{ mm}^2$ ) were prepared from the master alloy ingots by a single-roller melt-spinning apparatus. In situ high-pressure and high-temperature isothermal energy-dispersive X-ray powder diffraction measurements were performed using synchrotron radiation at the MAX80 station, HASYLAB, in Hamburg, Germany.<sup>16,17</sup> The cubic sample assembly, encapsulated inside a boron nitride container, was compressed by six truncation anvils of tungsten carbide in a 250-ton hydraulic press. The pressure of the sample was calculated from the lattice constant of NaCl using

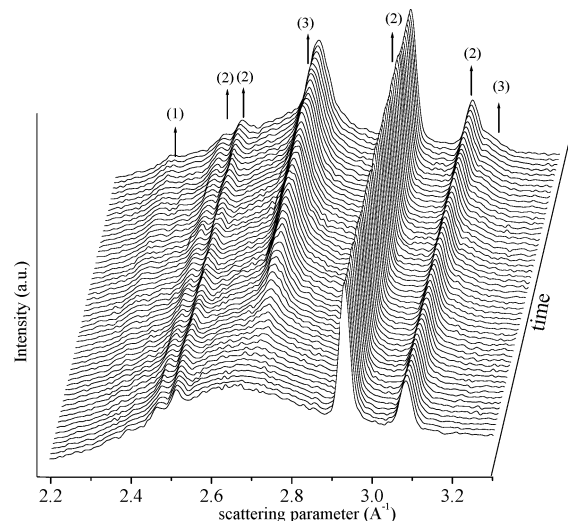


**Figure 1.** In situ EDXD patterns recorded at  $T = 190 \text{ }^\circ\text{C}$  and  $P = 0.1 \text{ GPa}$  for the  $\text{Al}_{89}\text{La}_6\text{Ni}_5$  amorphous alloy. The Bragg peaks labeled are from the bcc- $(\text{AlNi})_{11}\text{La}_3$ -like phase (1), from the boron nitride (2), and from the fcc Al crystal (3).

the Decker equation of state.<sup>18</sup> The heating was carried out by an electric current sent through a graphite heater via two appropriate anvils. The temperature was measured by means of a thermocouple voltage with a stability of  $\pm 1 \text{ K}$ . Each isothermal run consisted of a compression of the sample to a given pressure, followed by rapid isobaric heating to the working temperature (with an overshoot below  $2 \text{ K}$ ).

The sample was then kept at this temperature and irradiated by a polychromatic synchrotron beam. The EDXD patterns were collected in sequence for 3 min, each automatically recorded and stored. Pure Zr, Fe, and the metallic glass were used to examine the possible oxidation of the samples during the heat treatments using the sample assembly.

## 3. Results and Discussion

It was found that after heat treatments at temperatures up to  $600 \text{ }^\circ\text{C}$  only pure metallic phases in the three systems were detected. The structural evolution of the sample was performed at various pressures and temperatures.

As an example of the EDXD pattern collections, the sequences corresponding to  $T = 190 \text{ }^\circ\text{C}$  and  $P = 0.1 \text{ GPa}$  are shown in Figure 1 in the form of a 3-D map. Beside the Bragg peaks of the boron nitride (at  $q = 2.46, 2.51, 2.93,$  and  $3.08 \text{ } \text{\AA}^{-1}$ ), the characteristic features of the crystallization process are recorded. In accordance with the modality of crystallization proposed,<sup>8</sup> the main crystalline peak, around  $q = 2.71 \text{ } \text{\AA}^{-1}$ , and the secondary peak at  $q = 3.13 \text{ } \text{\AA}^{-1}$  are indexed to a fcc structure while the crystalline peak appearing at  $q = 2.34 \text{ } \text{\AA}^{-1}$  is associated with a metastable bcc- $(\text{AlNi})_{11}\text{La}_3$ -like phase (with lattice constant  $6.64 \text{ } \text{\AA}$  and space group  $Im3m$ ).<sup>8</sup>

Processing this sequence according to the DCE theory,<sup>10</sup> a transition parameter  $x(t)$  can be calculated as a function of time (Figure 2a). It is proportional to the entropy change of the system upon the phase transformations and its derivative  $dx(t)/dt$  (entropy change rate, in Figure 2b) corresponds to a DSC thermogram. The positions of the two maxima of the

- (10) Nishikawa, K.; Iijima, T. *Bull. Chem. Soc. Jpn.* **1984**, *57*, 1750.  
 (11) Caminiti, R.; Isopo, A.; Orru', M. A.; Rossi Albertini, V. *Chem. Mater.* **2000**, *12*, 369.  
 (12) Baranyai, A.; Evans, D. *Phys. Rev. A* **1990**, *42*, 849.  
 (13) Wallace, D. C. *J. Chem. Phys.* **1987**, *84*, 2282.  
 (14) Caminiti, R.; Rossi Albertini, V. *Int. Rev. Phys. Chem.* **1999**, *18*, 263.  
 (15) Rossi Albertini, V.; Bencivenni, L.; Caminiti, R.; Cilloco, F.; Sadun, C. *J. Macromol. Sci., Phys.* **1996**, *35*, 199.  
 (16) Jiang, J. Z.; Olsen, J. S.; Gerward, L.; Abdali, S.; Eckert, J.; Schlorke-de Boer, N.; Schultz, L.; Shi, P. X. *J. Appl. Phys.* **2000**, *87*, 2664.  
 (17) Olsen, J. S.; Gerward, L.; Jiang, J. Z. *J. Phys. Chem. Solids* **1999**, *60*, 229.

- (18) Decker, D. L. *J. Appl. Phys.* **1971**, *42*, 3239.

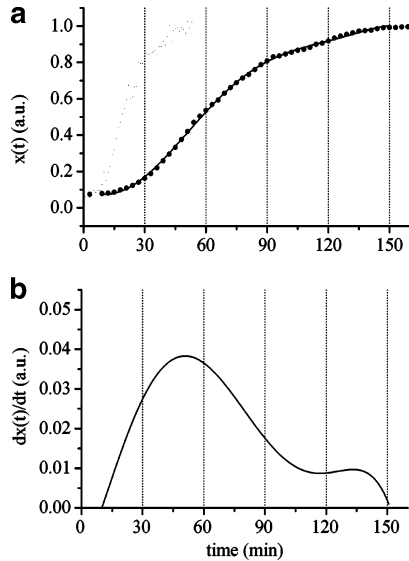


**Figure 2.** Transition parameter  $x(t)$ , proportional to the entropy change (a) experienced by the system during the phase transformation, and its derivative  $dx(t)/dt$  (proportional to the entropy change rate) (b) deduced from the EDXD patterns recorded at  $T = 190\text{ °C}$  and  $P = 0.1\text{ GPa}$  for the  $\text{Al}_{89}\text{La}_6\text{Ni}_5$  amorphous alloy.

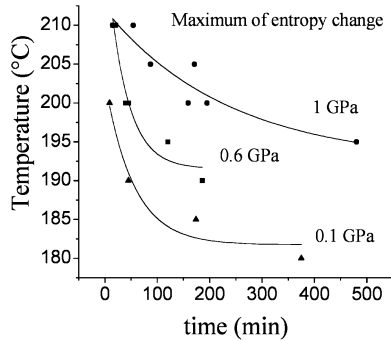


**Figure 3.** PTTT diagram points related to the first maximum of the entropy change and to the onset of the crystallization process for  $\text{Al}_{89}\text{La}_6\text{Ni}_5$  amorphous alloy.

$dx(t)/dt$  depend on the  $(P, T)$  values at which each sequence was acquired. Data points corresponding to the time at which  $dx(t)/dt$  reaches its maximum value can therefore be plotted as a function of the choice of  $P$  and  $T$  (while the time at which  $dx(t)/dt$  is 10% of its maximum value was assumed as the onset of the crystallization process). The PTTT diagram of the amorphous  $\text{La}_6\text{Ni}_5\text{Al}_{89}$  alloy is depicted in Figure 3. Here, the time required for crystallization decreases with increasing temperature, while the time required for the transition increases with increasing pressure; i.e., the pressure applied to the sample retards the crystallization process.

The former DCE results are consistent with DSC measurements, performed at ambient pressure at both  $T = 200\text{ °C}$  and  $T = 190\text{ °C}$ . They are compared with the  $dx(t)/dt$  deduced from the EDXD patterns (recorded at  $T = 190\text{ °C}$  and  $P = 0.1\text{ GPa}$ ) in Figure 4. The results are summarized in Figure 5, demonstrating that the time required for the  $dx(t)/dt$  to reach its (first) maximum becomes larger when an external pressure is applied (and that the first crystallization in amorphous  $\text{La}_6\text{Ni}_5\text{Al}_{89}$  is retarded, as mentioned above). This pressure dependence has been fitted in terms of an exponential growth to extrapolate the time at which the maximum  $dx(t)/dt$  would be reached at ambient pressure, at

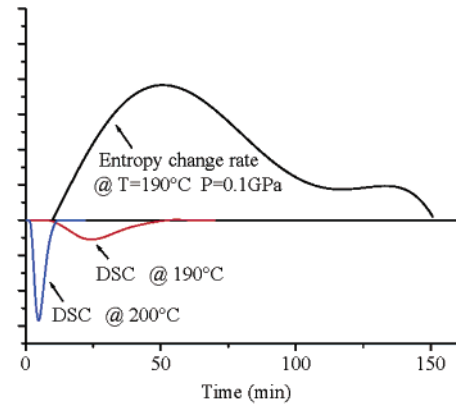


**Figure 4.** Comparison of the entropy change rate (a) deduced from the EDXD patterns (recorded at  $T = 190\text{ °C}$  and  $P = 0.1\text{ GPa}$ ) and the DSC curves recorded at ambient pressure and at  $T = 200\text{ °C}$  and  $T = 190\text{ °C}$ , respectively.

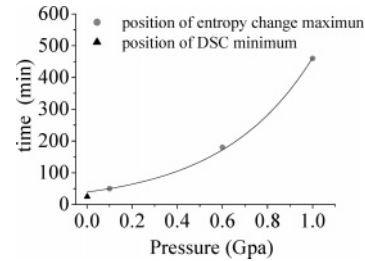


**Figure 5.** Pressure dependence of the position of the entropy change rate is in agreement with the position of the DSC minimum.

which the DSC measurements were executed. The graph illustrates that, also in the case of amorphous alloys, a good agreement between the DSC and the DCE measurements is found.

The results so obtained (in Figure 3) can be discussed on the basis of the pressure dependence of the thermodynamic potential barrier and of the diffusion activation energy.

Indeed, the crystallization of an amorphous alloy proceeds through an initial nucleation process, followed by the crystal growth. The crystallization temperature  $T_x$  of the alloy is governed by the potential barrier of nucleation and the diffusion activation energy. Therefore, the behavior of  $T_x$  as a function of  $P$  can be interpreted in terms of the pressure dependence of the nucleation work:  $(\Delta G^* + Q_n)$ , where  $\Delta G^*$  is the free energy required to form a nucleus of the critical size and  $Q_n$  is the activation energy for the transport of an atom across the interface of an embryo. Homogeneous nucleation  $\Delta G^*$ , at a given pressure, is defined as

$$\Delta G^*(T, P) = \frac{16\pi\sigma^3(V_m^c)^2}{3[P(V_m^a - V_m^c) - (\Delta G^{a \rightarrow c}(T, P) + E)]^2} \quad (1)$$

where  $V_m^c$  and  $V_m^a$  are the molar volumes of the crystalline and amorphous phases,  $E$  is the elastic energy induced by the volume change,  $\sigma$  is the interfacial energy, and  $\Delta G^{a \rightarrow c}$  is the molar free energy change for the amorphous to crystalline phase transformation.

The pressure dependence of the nucleation work,  $\Delta G^* + Q_n$ , under general assumptions is discussed in ref 8. Referring to Figure 6, we can define a threshold pressure  $P^*$  at which the nucleation work increases with pressure, so that it is dominated by  $\Delta G^*$  below  $P^*$  and by  $Q_n$  above it.

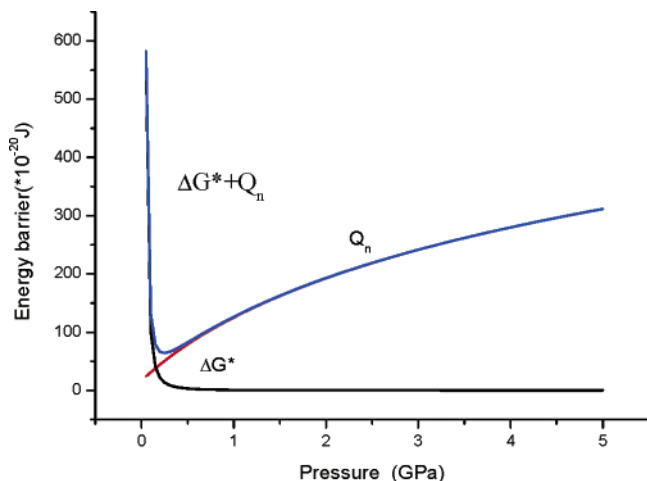


**Figure 6.** Schematic illustration of the pressure dependences of  $\Delta G^*$ ,  $Q_n$ , and  $\Delta G^* + Q_n$ .

The result of the present measurements indicates that, in the present isothermal conditions (heating rate vanishingly small),  $P^*$  is below 0.1 GPa, i.e.,  $T_x$  is an increasing function of the pressure in all the range explored, as shown in Figure 3.

### Conclusions

In summary, we present in situ high-pressure and high-temperature DCE measurements of an amorphous  $\text{La}_6\text{Ni}_5$

$\text{Al}_{89}$  alloy upon crystallization in the pressure range of 0.1–1 GPa. Some points of the pressure–time–temperature transformation diagram of the first crystallization in an amorphous  $\text{La}_6\text{Ni}_5 \text{Al}_{89}$  alloy were obtained. It was found that the time required for the transition increases with increasing pressure, a result that was analyzed on the basis of the dependence of the thermodynamic potential barrier and of the diffusion activation energy from the applied pressure.

Besides the useful information retrieved on the crystallization processes of the amorphous alloy, the results reported demonstrate that the original DCE technique is an appropriate tool to perform phase transition measurements in extreme conditions (very small samples submitted to high-temperature/-pressure conditions) when the DSC method fails.

**Acknowledgment.** The authors would like to thank BSRF in Beijing, NSRL in Hefei, HASYLAB in Hamburg SPring8 and KEK in Japan for use of the synchrotron radiation facilities and Mr. A. Casling for his critical reading of the manuscript. Financial support from the National Natural Science Foundation of China (Grant Nos. 50341032 and 50425102), the Ministry of Science and Technology of China (Grant Nos. 2004/249/37-14 and 2004/250/31-01A), the Ministry of Education of China, and Zhejiang University is gratefully acknowledged.

CM051547L